WILEY-VCH

Strain-induced Ring Expansion Reactions of Calix[3]pyrrole-related Macrocycles

Yuya Inaba,[a] Yu Kakibayashi,[a] Yuki Ide,[b] Jenny Pirillo,[b] Yuh Hijikata,*[b] Tomoki Yoneda,[a] and Yasuhide Inokuma*[a,b]
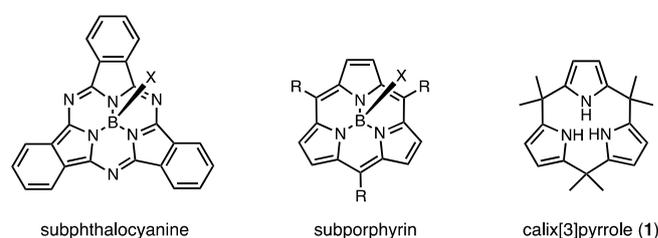
[a]   Y. Inaba, Y. Kakibayashi, Dr. T. Yoneda, Prof. Dr. Y. Inokuma
        Division of Applied Chemistry, Faculty of Engineering
        Hokkaido University
        Kita 13, Nishi 8, Kita-ku, Sapporo, Hokkaido, 060-8628, Japan
        E-mail: inokuma@eng.hokudai.ac.jp
[b]   Dr. Y. Ide, Dr. Y. Hijikata, Prof. Dr. Y. Inokuma
        Institute for Chemical Reaction Design and Discovery (WPI-ICReDD)
        Hokkaido University
        Kita 21, Nishi 10, Kita-ku, Sapporo, Hokkaido, 001-0021, Japan
        E-mail: hijikata@icredd.hokudai.ac.jp

        Supporting information of this article can be found under:

Abstract: The recent discovery of calix[3]pyrrole, a porphyrinogen-like tripyrrolic macrocycle, has provided an unprecedented strain-induced ring expansion reaction into calix[6]pyrrole. Here, we synthesized calix[n]furan[3–n]pyrrole (n = 1~3) macrocycles to investigate the reaction scope and mechanism of the ring expansion. Single crystal X-ray analysis and theoretical calculations revealed that macrocyclic ring strain increases as the number of inner NH sites increases. While calix[1]furan[2]pyrrole exhibited almost quantitative conversion into calix[2]furan[4]pyrrole within 5 minutes, less-strained calix[2]furan[1]pyrrole and calix[3]furan were inert. However, N-methylation of calix[2]furan[1]pyrrole induced a ring-expansion reaction that enabled the isolation of a linear reaction intermediate. The mechanism analysis revealed that the ring expansion consists of regioselective ring cleavage and subsequent cyclodimerization. This reaction was further utilized for synthesis of calix[6]-type macrocycles.

Introduction

While naturally occurring porphyrins that consist of four pyrrole units connected with four *meso*-carbon atoms are more common, their ring-contracted analogs with three pyrrole units have gathered more attention because of their unique structural and electronic properties.[1] For example, subphthalocyanines[2] and subporphyrins[3] have bowl-shaped 14π-aromatic macrocycles that show visible light absorption/emission,[4] photo-induced electron-transfer,[5] and host-guest interactions using concave-to-convex type π-stacking.[6] Most tripyrrolic porphyrin and phthalocyanine analogs have been synthesized as boron(III)-complexes,[7] and are chemically stable enough to be handled in strong acid or base owing to the boron-chelation effect.[8]

Recently, our group achieved template-free synthesis of calix[3]pyrrole (**1**)[9] (Figure 1), a porphyrinogen-like tripyrrolic macrocycle with three sp^3-carbon bridges, using a hexaketone precursor. Unlike subporphyrins, macrocycle **1** has a short life-time (<10 seconds) under acidic conditions conventionally used

for porphyrin synthesis,[10] and quantitatively converts into calix[6]pyrrole to release the macrocyclic ring strain. This ring-expansion reaction has explained a long-standing question, why pyrrole monomers selectively form tetrapyrrolic macrocycles, whereas the corresponding tripyrrolic macrocycles are never observed.

**Figure 1.** Contracted porphyrin-related macrocycles with three pyrrole units.

Among known macrocyclic ring expansion or contraction reactions of porphyrinoids,[11] twofold expansion of the ring size is quite rare yet promising for the synthesis of larger macrocycles. However, its detailed mechanism and reaction scope are still unclear. In this work, we synthesized calix[n]furan[3–n]pyrroles (n = 1~3) as calix[3]pyrrole-related macrocycles having different ring strain energies, and investigated the substrate scope and reaction mechanism of their strain-induced ring expansion reactions. Ring strain of these macrocycles was analyzed using theoretical calculations and deformation angles obtained from crystal structures. We determined that ring strain energy tends to increase as the number of inner NH sites increases. Under acidic conditions, calix[1]furan[2]pyrrole (**2**) underwent regioselective ring cleavage and conversion into calix[2]furan[4]pyrrole, similar to previously observed for calix[3]pyrrole (**1**), whereas less-strained calix[2]furan[1]pyrrole (**3**) and calix[3]furan (**4**) were stable under similar conditions. N-methylation of calix[2]furan[1]pyrrole, however, impelled the ring expansion reaction and enabled the isolation of a linear reaction intermediate.

Further scrambling experiments and theoretical calculations revealed a plausible reaction mechanism that included regioselective C–C bond cleavage and cyclodimerization of linear intermediates. Furthermore, we demonstrated synthetic access to novel calix[6]-type macrocycles using strain-induced ring expansion that were otherwise difficult to access using conventional methods.

Results and Discussion

As illustrated in Scheme 1, syntheses of calix[3]-type macrocycles **2** and **3** began with intramolecular cyclization of linear hexaketone precursor **5**[12] to obtain difuran macrocycle **6**, which was analogous to calix[3]pyrrole synthesis.[9] While treatment of **6** with 5.0 equiv. of *m*-chloroperbenzoic acid (*m*CPBA) furnished cyclic hexaketone in 28% as a result of double ring opening, use of 3.0 equiv. of *m*CPBA provided mono-furan macrocycle **7** in 71% yield after the reduction of enedione intermediate with zinc. Paal–Knorr type pyrrole formation reaction on **7** with ammonium acetate in refluxing ethanol gave calix[1]furan[2]pyrrole (**2**) in 67% yield. In a similar fashion, calix[2]furan[1]pyrrole (**3**) was obtained in 79% yield from diketone macrocycle **6** under Paal–Knorr conditions. As a more hindered analog, *N*-methylated derivative **3-Me** was synthesized by treatment of **3** with sodium hydride and methyl iodide in 82% yield. Synthetic yield of calix[3]furan (**4**) was improved to be 53%, when P_2O_5 was added as a dehydrating agent to the previously reported conditions (42%)[9].
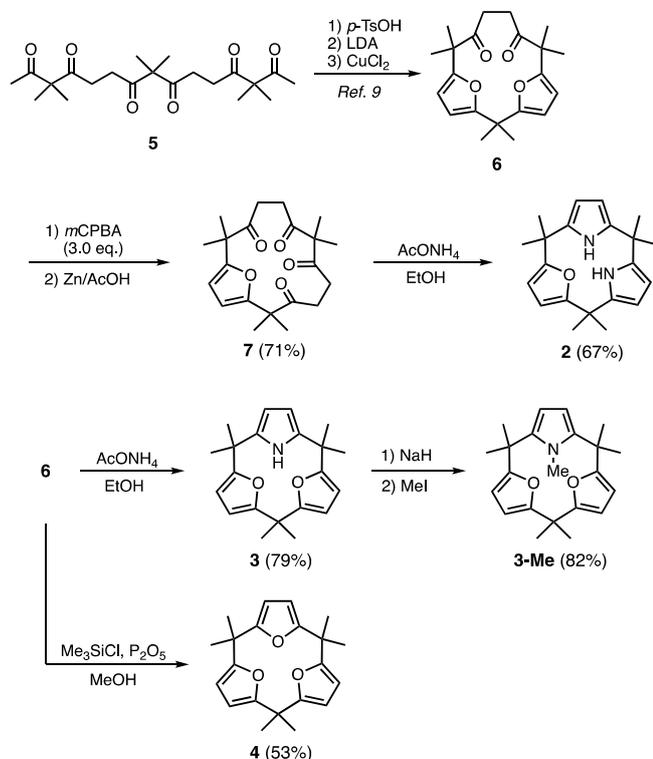
Scheme 1. Synthesis of calix[3]pyrrole analogs.

^{1}H NMR spectrum of **2** in chloroform-*d* ($CDCl_3$) exhibited a single set of pyrrole proton signals at 6.98 (NH), 5.96 (*β*-CH), and 5.86 (*β*-CH) ppm and three singlets at 5.87, 1.60, and 1.57 ppm, which were assignable to furan and the two types of dimethylmethylene groups, respectively. The observed signal pattern indicated time-averaged C_{2v} molecular symmetry for **2** in solution. The same molecular symmetry was observed in the ^{1}H NMR spectrum of **3**, in which remarkable down-field-shifted pyrrole NH proton was observed at 10.34 ppm, presumably because of the ring-current effect of furan rings and weak hydrogen bonding interactions. Meanwhile, methylated analog **3-Me** showed C_s symmetric ^{1}H NMR signal pattern represented by four different signals for dimethylmethylene parts at 1.66, 1.63, 1.57, and 1.48 ppm. Two geminal methyl groups became diastereotopic upon *N*-methylation of **3**, which indicated that the flipping motion of the *N*-methylpyrrole unit in **3-Me** is slow on the NMR time scale. The split signal of dimethylmethylene parts of **3-Me** did not coalesce even at 100 °C in dimethyl sulfoxide-d_6.
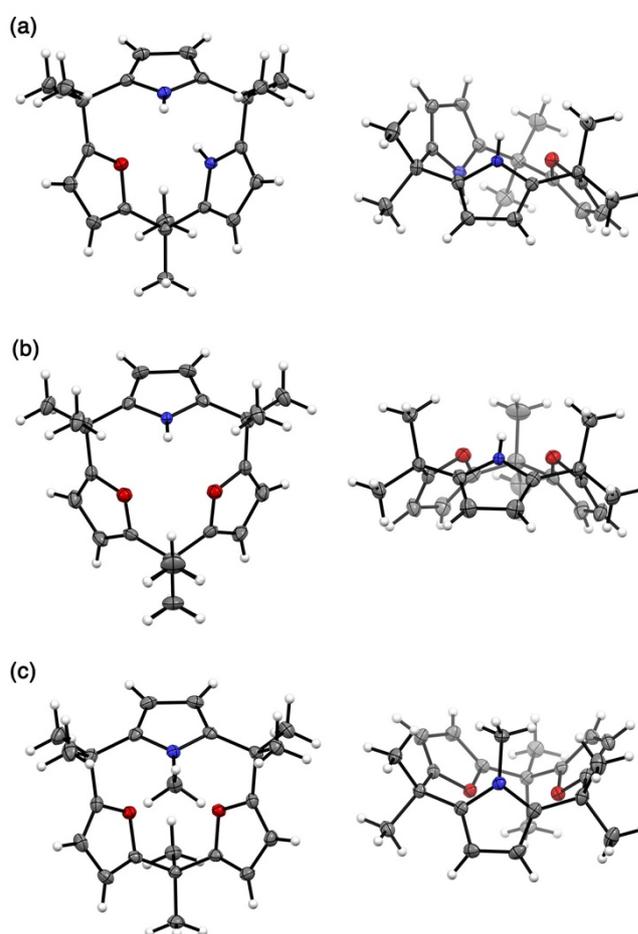
Figure 2. Single crystal X-ray structures of (a) **2**, (b) **3**, and (c) **3-Me** (left: top view, right: side view). Thermal ellipsoids are drawn at the 50% probability level (C: gray; N: blue; O: red; H: white).

Single crystal X-ray diffraction analysis unambiguously determined the macrocyclic structures of **2**, **3**, and **3-Me** (Figure 2). Calix[1]furan[2]pyrrole (**2**) crystallized as a hemihydrate form in a similar packing fashion as previously reported for **1**. One of the two pyrrole N-H sites was hydrogen-bonded to co-crystallized water molecule (see Supporting Information; SI). The other N-H

site was on the opposite side of the macrocycle, on the same side as the furan oxygen atom. The crystal structure of calix[2]furan[1]pyrrole (**3**) exhibited a cone-shape conformation in which all the hetero atoms were placed on the same side of the macrocycle. Similar cone-shape conformation was also observed for less-hindered calix[3]furan (**4**),[9] suggesting that steric hindrance between inner N-H sites in **2** was released by replacement with an oxygen atom. In contrast, the *N*-methylated analog **3-Me** exhibited a non-cone-shaped conformation similar to those for **1** and **2**. Dihedral angles between the mean plane of three *meso*-carbon atoms and pyrrole ring in **3-Me** was 74.1°, which was remarkably larger than that of **3** (44.7°), reflecting significant steric hindrance of the *N*-methyl group.

Macrocyclic ring strain of the calix[3]pyrrole analogs was evaluated by deformation angles around the aromatic units.[13] Deformation angle α represents deformation of pyrrole or furan rings from planarity, and deformation angle β shows displacement of the *meso*-carbon atom from the bow of the heteroaromatic ring. We observed that the deformation angles around pyrrole rings of **1–3** decreases as the number of N-H sites decreases (Table 1). Changes in the deformation angles β (3.03° between **1** and **3**) were more apparent than those in α (0.04° between **1** and **3**), indicating that the displacement of *meso*-carbon atoms next to a pyrrole unit is more susceptible to ring strain. The impact of *N*-methylation on **3** appeared on the deformation angle β; **3-Me** exhibited the largest deformation angle β of 11.70° in the series. While the smallest deformation angle α of 2.03° was observed for the *N*-methylpyrrole unit, this is still significantly larger than that of calix[4]pyrrole (α = 0.38°).[14] Deformation angles around furan rings in **2**, **3**, **3-Me**, and **4** were relatively smaller than those for pyrroles, and no obvious correlation was seen between these angles and number of pyrrole units.

Table 1. Averaged deformation angles[a] for pyrrole and furan units for calix[3]pyrrole analogs **1–3**, **3-Me**, and **4**.

	1	2	3	3-Me	4
Pyrrole α (°)	2.52	2.49	2.48	2.03	
Pyrrole β (°)	9.20	8.52	6.17	11.70	
Furan α (°)		2.14	2.31	1.91	1.95
Furan β (°)		5.78	7.15	5.49	6.53

[a] Deformation angles α and β for each heteroaromatic ring are defined by the averaged deviation angles between the mean planes of X−C(3)−C(4) and X−C(2)−C(3), and the mean plane X−C(2)−C(3) and a C(2)−C(*meso*) bond, respectively. (X = N or O).
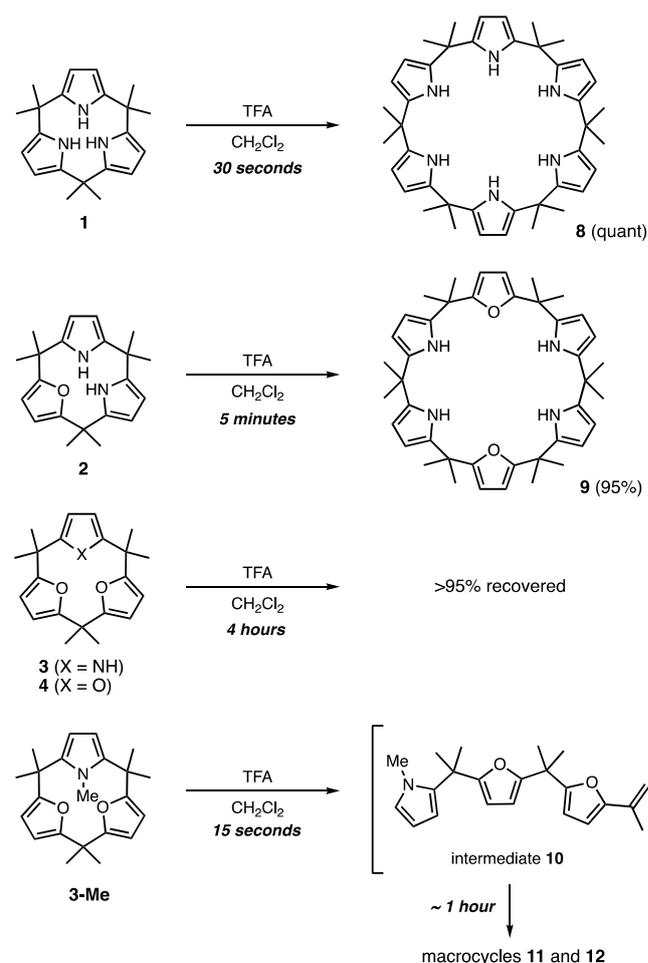
Table 2. Calculated macrocyclic ring strain energy[a] for **1–4**.

|	1	2	3	3-Me	4
Strain energy (kcal/mol)	-20.0	-17.7	-12.2	–[b]	-16.4

[a] Strain energies were estimated from energy difference between the linear and cyclic forms of **1–3**, **3-Me**, and **4** (see SI for the detailed conditions). Negative values indicate that linear forms are more stable than cyclic forms. [b] Although the strain energy of **3-Me** was calculated to be −10.4 kcal/mol using the same method, the value could be affected by factors such as dispersion interaction and change of charge distribution caused by the N-Me group, which

induces stabilization of the strained ring form indicated by large β and makes it difficult to compare with the ring strain energy of the other compounds.

A similar tendency of ring strain energies for **1–3**, **3-Me**, and **4** was also revealed by theoretical calculations at the B3LYP/cc-pVTZ level of theory, including the Grimme-type dispersion correction and solvation effect by the polarizable continuum model (solvent = CH_2Cl_2) using Gaussian 16 Rev. C.01.[15] When formation energies of the oligopyrrole/furan sequences in **1–3**, **3-Me**, and **4** were compared between their cyclic and linear forms (see SI), **1** showed the largest strain energy of 20.0 kcal/mol (Table 2). Ring strain energy tends to decrease as the number of inner N-H groups decreases because steric repulsion at the central area of the rings also decreases, while **4** has higher strain-energy due to the electrostatic repulsion among oxygen atoms. In the case of **3-Me**, the linear form was less stable because of steric repulsion between the *N*-substituted methyl group and the dimethylmethylene parts. In addition, the *N*-substituted methyl group induced dispersion interaction with the surrounding parts and changes in the atomic charges that stabilize the system in the ring form. On the basis of these factors, it seems difficult to compare the strain energy of **3-Me** with that of compounds **1–4**.

Scheme 2. Strain-induced ring expansion reactions of calix[3]pyrrole analogs.
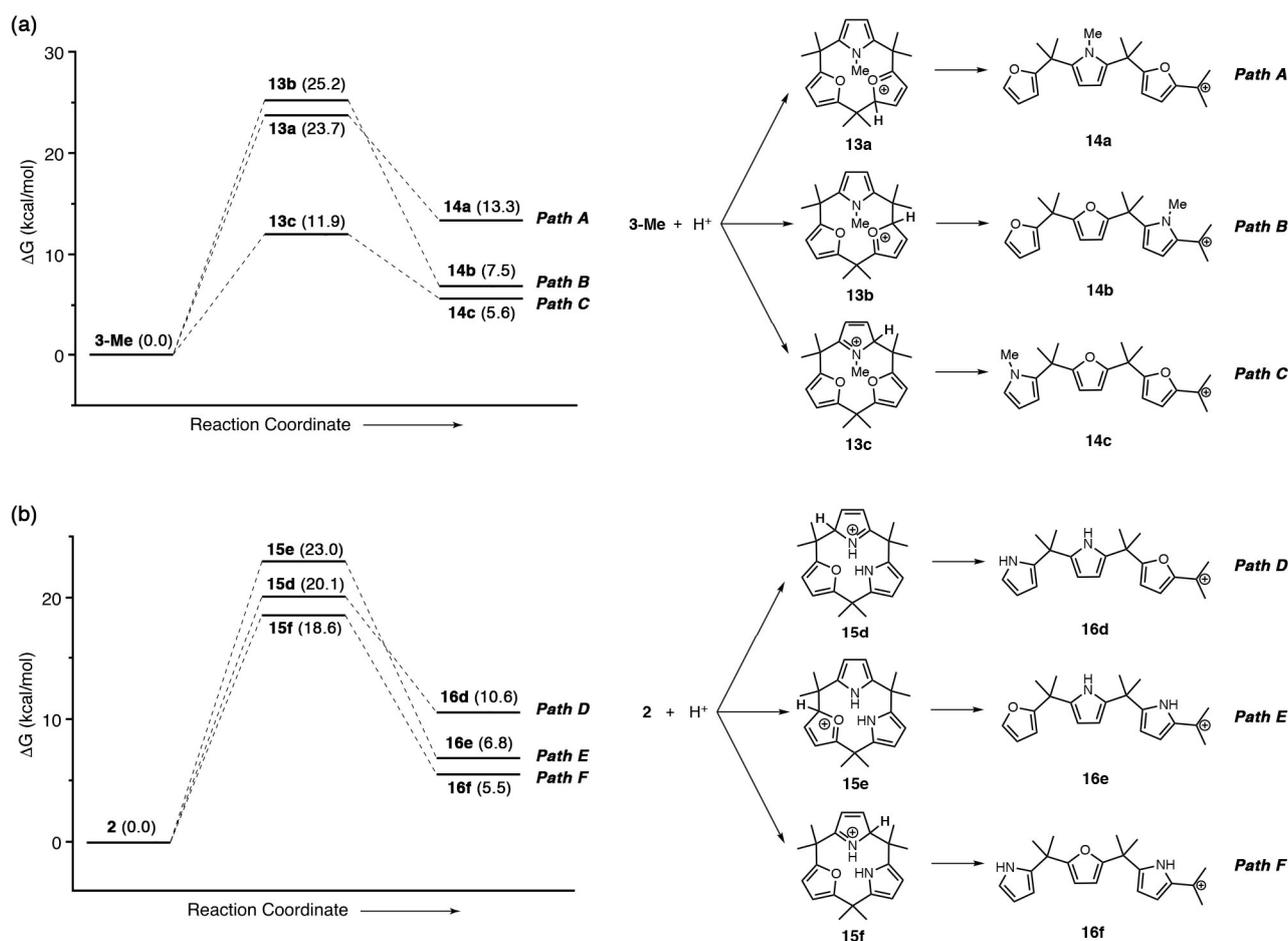
Figure 3. Relative free energy diagrams of possible pathways for macrocyclic ring cleavage step of (a) **3-Me** and (b) **2** calculated at the B3LYP/cc-pVTZ level of theory including dispersion correction and IEFPCM (CH₂Cl₂). TFA was used as a proton source.

Macrocyclic ring strain made significant differences in the ring-expansion reaction under acidic conditions. When **1** was dissolved in a 10 mM dichloromethane solution of trifluoroacetic acid (TFA) at room temperature (so-called Rothemund–Lindsey conditions[10]), tripyrrolic macrocycle **1** completely disappeared and calix[6]pyrrole (**8**) was quantitatively formed within 30 seconds (Scheme 2).[9] Under the same reaction conditions, calix[1]furan[2]pyrrole (**2**) furnished calix[2]furan[4]pyrrole (**9**) over 5 minutes in 95% yield. Conversion of the starting material **2** became slower than that of **1** as a result of the reduced strain energy. Interestingly, product **9** was obtained with a perfect regioselectivity; no other regioisomers were observed in the NMR spectrum of the reaction mixture, although calix[2]furan[4]pyrrole can have three regioisomers depending on the positions of furan rings. This implied that macrocyclic ring cleavage, which is likely an initial step of the ring-expansion reaction, occurred in a regioselective fashion on macrocycle **2**. In contrast, more than 95% of **3** was recovered even after 4 hours stirring in the presence of TFA. Although the parent ion peaks for expected calix[4]furan[2]pyrrole were observed in the electrospray ionization time-of-flight (ESI-TOF) mass spectrum of the reaction mixture (see SI), isolation was unsuccessful because of the presence of unassignable byproducts with similar retention times on the high-performance liquid chromatography (HPLC) chromatogram. Calix[3]furan (**4**) was also inert under these conditions, although **4** is known to undergo hydrolysis of a furan

ring to give **6** under aqueous conditions (stirring in a mixture of ethanol and 12 M hydrochloric acid for 30 hours).[9]

While **3** was inert under the Rothemund–Lindsey conditions, its *N*-methylated analog **3-Me** was completely converted within 1 minute in the presence of TFA. Unlike **1** and **2**, an intermediate **10** that had the same molecular formula as **3-Me** was observed at earlier times (~5–30 seconds) from liquid chromatography–mass spectrometry (LC-MS) analysis. Remarkably, intermediate **10** was successfully isolated by quenching of the reaction at 30 seconds, and characterized to be a linear structural isomer of **3-Me**. The ¹H NMR spectrum of **10** showed pyrrole α-CH proton at 6.44 ppm in CDCl₃. Two olefinic protons for the 2-propenyl group were observed at 5.37 and 4.86 ppm, which showed NOE correlation with a furan β-CH proton on the 2-dimensional NMR spectrum. Formation of intermediate **10** can be reasonably explained as follows: (1) the pyrrole unit underwent protonation at the α-position, (2) the C(protonated pyrrole-α)–C(*meso*) bond was dissociated to give tertiary carbocation and an α-free pyrrole ring, and (3) deprotonation at a methyl group next to the carbocation center resulted in the formation of the 2-propenyl group.

The observed regioselectivity in ring cleavage of **3-Me** is also supported by theoretical calculations. Considering the protonation sites on **3-Me**, we postulated three possible pathways for macrocyclic ring cleavage step (Paths A to C in Figure 3).

Energy calculations at the B3LYP/cc-pVTZ level of theory indicated that the pyrrole-protonated cation **13c** formed in Path C was over 11.8 kcal/mol more stable than the other furan-protonated cations **13a** and **13b**. This is reasonable because pyrrole is more electron-rich than furan. Furthermore, linear cation species **14c** in Path C was found to be more stable than **14a** and **14b** in Paths A and B. As a result, Path C was the most favorable among the three paths. In fact, the isolated intermediate **10** was regarded as a deprotonated form of **14c** in Path C.

In a similar fashion, we also theoretically investigated the macrocyclic ring cleavage step for **2**. While the furan-protonated cation **15e** in Path E had the largest ΔG, the energy difference between the two pyrrole-protonated cations **15d** and **15f** was only 1.5 kcal/mol. However, linear cation **16d** formed in Path D was 5.1 kcal/mol less stable than **16f** in Path F, because of the less electron-donating character of furan ring for the neighboring carbocation center. Therefore, Path F in which C(pyrrole-α)–C(*meso*) bond cleavage occurs between the two pyrrole units seems the most realistic pathway.

Further experimental evidence for the regioselective ring cleavage was obtained by a scrambling experiment (Scheme 3). When a strain-induced ring expansion reaction was conducted with a 1:1 mixture of **1** and **2**, the cross-coupled product calix[1]furan[5]pyrrole (**17**) was formed in 35% yield along with homo-dimers **8** and **9**. Importantly, no other regioisomer was found in the reaction mixture, indicating exclusive formation of linear intermediate such as **16f** from **2**.
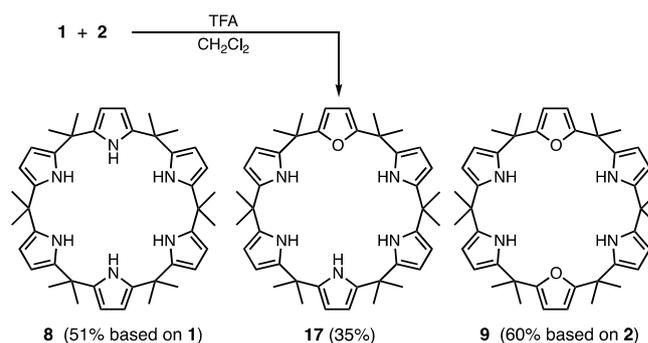

**Scheme 3.** Scrambling experiment between **1** and **2**.

A reasonable reaction mechanism for the strain-induced ring expansion reaction of calix[3]pyrrole analogs is described in Scheme 4. The reaction consists of two steps: macrocyclic ring cleavage and subsequent cyclodimerization of linear intermediates. In the first step, protonation at an electron-rich pyrrole α-carbon atom triggers the regioselective C(pyrrole-α)–C(*meso*) bond cleavage to release the macrocyclic ring strain. Linear cation intermediate (electrophile) thus generated can reversibly form a 2-propenyl-substituted tripyrrane analog (nucleophile) through deprotonation/protonation. An aromatic electrophilic substitution reaction between carbocation and an α-free pyrrole unit gives a hexapyrrane-like species that undergoes intramolecular macrocyclization to give calix[6]pyrrole-analogs such as **8** and **9**. It should be emphasized that intramolecular macrocyclization of tripyrrane analogs is very slow compared with that of hexapyrrane because of the short chain length.

The strain-induced ring expansion reaction can be applied for a unique synthesis of novel calix[6]-type macrocycles. When the reaction of **3-Me** with TFA was monitored for 1 hour, intermediate **10** completely disappeared and several peaks correspond to cyclic oligomers of **10** were detected by LC-MS analysis. The major HPLC fraction contained two isomers of calix[4]furan[2]*N*-methylpyrrole, **11** and **12**, in 32% and 18%
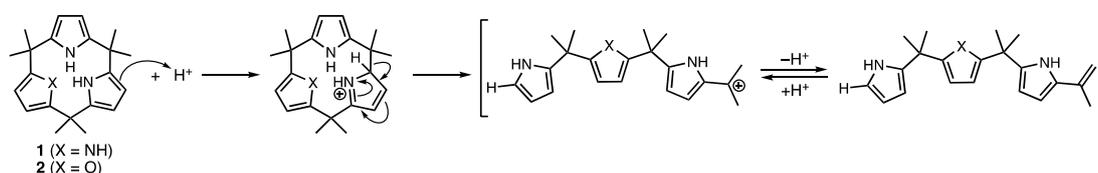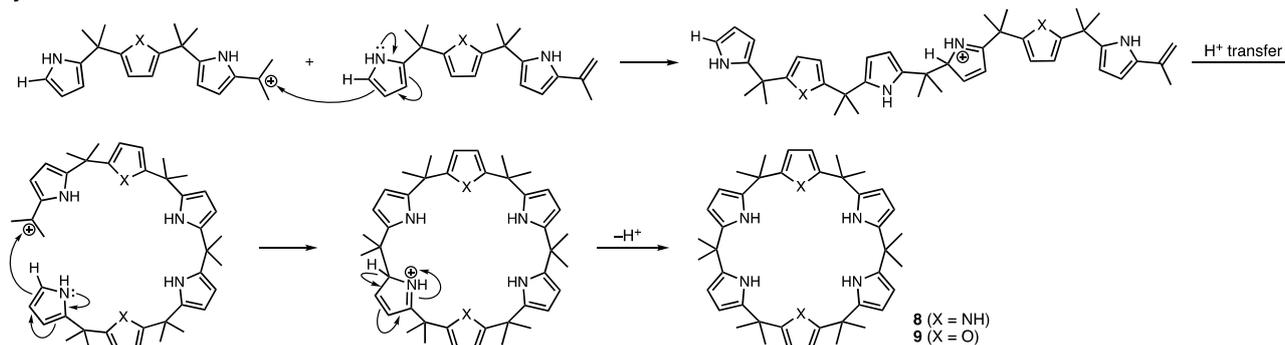
Scheme 4. Proposed reaction mechanism for strain-induced ring expansion of **1** and **2**.

yields, respectively. Single crystal X-ray diffraction analysis revealed the structure of **11** as doubly *N*-confused calix[4]furan[2]*N*-methylpyrrole with C_{2h} molecular symmetry (Figure 4). Another product **12** was found to be a structural isomer of **11** with C_{2v} molecular symmetry. Both macrocycles exhibited parallelogram-like conformations in which two furan units were inverted. Although other minor HPLC fractions suggested formation of larger macrocycles such as calix[6]furan[3]*N*-methylpyrrole and calix[8]furan[4]*N*-methylpyrrole (Figure S12), the existence of several structural isomers derived from C(pyrrole-β)–C(*meso*) linkage hampered their isolation. While the α-position of pyrrole is more electron-rich, rearrangement of the α-substituent to the β-position is known for *N*-substituted pyrroles under acidic conditions.[16] For a similar reason, steric repulsion between the *N*-methyl group and the nearby dimethylmethylene unit have rendered *N*-confused macrocycles **11** and **12** thermodynamically favored over an all α-substituted isomer. Such steric repulsion would be critical for the isolation of linear intermediate **10**, which is otherwise elusive for the reactions with **1** and **2** because of rapid dimerization.
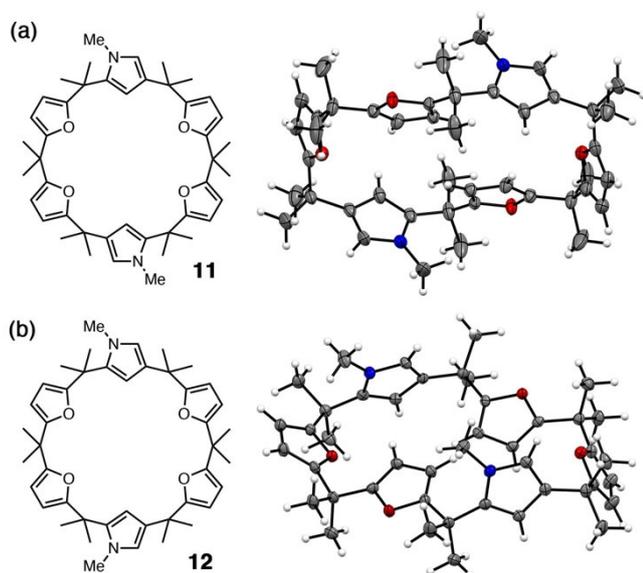
12. Successful isolation of the linear intermediate **10** and theoretical calculations provided a plausible reaction mechanism that was also verified by a scrambling experiment. The present results clearly show unique reactivities of calix[3]pyrrole-type macrocycles that were inaccessible via condensation reactions of pyrroles. Moreover, regioselective generation of highly reactive linear tripyrrane-like cations demonstrated the synthetic utility of calix[3]pyrrole analogs for the synthesis of expanded macrocycles. In conventional methods, calix[6]-type macrocycles[17] such as **8**, **9**, and **17** have so far been synthesized through multistep synthesis that involves time-consuming chromatographic separation processes. The present approach using strain-induced ring expansion can facilitate efficient generation of calix[6]-type macrocycles, especially those with two or more different aromatic units.

Experimental Section

Figure 4. Single crystal X-ray structures of **11** and **12**.

Acknowledgements

Conflict of Interest

The authors declare no conflict of interest.

Conclusion

In conclusion, we demonstrated oligoketone-based synthesis of calix[3]pyrrole analogs, calix[*n*]furan[3–*n*]pyrroles (*n* = 1~3), with various macrocyclic ring strain energies. Deformation angle analysis using X-ray crystal structures revealed that displacement of *meso*-carbon atoms next to a pyrrole ring became more pronounced as the number of inner N-H sites increased. While calix[1]furan[2]pyrrole (**2**) exhibited similar reactivity to that of calix[3]pyrrole (**1**) in the presence of TFA to give expanded macrocycle **9** almost quantitatively, the less-strained calix[2]furan[1]pyrrole (**3**) and calix[3]furan (**4**) were stable under such acidic conditions. Nevertheless, *N*-methylation of **3** increased the macrocyclic strain enough to trigger a ring expansion to doubly *N*-confused calix[6]-type macrocycles **11** and

[1]   a) C. G. Claessens, D. González-Rodríguez, T. Torres, *Chem. Rev.* **2002**, *102*, 835–854; b) T. Torres, *Angew. Chem. Int. Ed.* **2006**, *45*, 2834–2837; *Angew. Chem.* **2006**, *118*, 2900–2903; c) C. G. Claessens, D. González-Rodríguez, M. S. Rodríguez-Morgade, A. Medina, T. Torres, *Chem. Rev.* **2014**, *114*, 2192–2277; d) S. Shimizu, *Chem. Rev.* **2017**, *117*, 2730–2784; e) Y. Inokuma, A. Osuka, *Dalton Trans.* **2008**, 2517–2526.
[2]   A. Meller, A. Ossko, *Monatsh. Chem.* **1972**, *103*, 150–155.
[3]   a) Y. Inokuma, J. H. Kwon, T. K. Ahn, M.-C. Yoon, D. Kim, A. Osuka, *Angew. Chem. Int. Ed.* **2006**, *45*, 961-964; *Angew. Chem.* **2006**, *118*, 975–978; b) N. Kobayashi, Y. Takeuchi, A. Matsuda, *Angew. Chem. Int. Ed.* **2007**, *46*, 758–760; *Angew. Chem.* **2007**, *119*, 772–774.

[4]   a) Y. Takeuchi, A. Matsuda, N. Kobayashi, *J. Am. Chem. Soc.* **2007**, *129*, 8271–8281; b) Y. Inokuma, Z. S. Yoon, D. Kim, A. Osuka, *J. Am. Chem. Soc.* **2007**, *129*, 4747–4761. c) D. D. Díaz, H. J. Bolink, L. Cappelli, C. G. Claessens, E. Coronado, T. Torres, *Tetrahedron Lett.* **2007**, *48*, 4657–4660; d) N. Kobayashi, *J. Chem. Soc., Chem. Commun.* **1991**, 1203–1205; e) Y. Inokuma, S. Easwaramoorthi, Z. S. Yoon, D. Kim, A. Osuka, *J. Am. Chem. Soc.* **2008**, *130*, 12234–12235.

[5]   a) D. González-Rodríguez, T. Torres, M. M. Olmstead, J. Rivera, M. Á. Herranz, L. Echegoyen, C. A. Castellanos, D. M. Guldi, *J. Am. Chem. Soc.* **2006**, *128*, 10680–10681; b) B. Küçüköz, B. Adinarayana, A. Osuka, B. Albinsson, *Phys. Chem. Chem. Phys.* **2019**, *21*, 16477–16485.

[6]   a) C. G. Claessens, T. Torres, *Chem. Commun.* **2004**, 1298–1299; b) D. V. Konarev, S. I. Troyanov, R. N. Lyubovskaya, *CrystEngComm* **2015**, *17*, 3923–3926; c) K. Yoshida, A. Osuka, *Chem. Eur. J.* **2016**, *22*, 9396–9403.

[7]   Some core-modified analogues are known as boron-free forms: a) R. Myśliborski, L. Latos-Grażyński, L. Szterenberg, T. Lis, *Angew. Chem. Int. Ed.* **2006**, *45*, 3670–3674; *Angew. Chem.* **2006**, *118*, 3752–3756; b) D. Kuzuhara, H. Yamada, Z.-L. Xue, T. Okujima, S. Mori, Z. Shenc, H. Uno, *Chem. Commun.* **2011**, *47*, 722–724; c) S. B. Kumar, N. N. Pati, J. V. K. Jose, K. P. Panda, *Chem. Commun.* **2020**, *56*, 5637–5640.

[8]   a) T. Kato, F. S. Tham, P. D. W. Boyd, C. A. Reed, *Heteroat. Chem.* **2006**, *17*, 209–214; b) E. Tsurumaki, S. Hayashi, F. S. Tham, C. A. Reed, A. Osuka, *J. Am. Chem. Soc.* **2011**, *133*, 11956–11959.

[9]   Y. Inaba, Y. Nomata, Y. Ide, J. Pirillo, Y. Hijikata, T. Yoneda, A. Osuka, J. L. Sessler, Y. Inokuma, *J. Am. Chem. Soc.* **2021**, *143*, 12355–12360.

[10]   a) J. S. Lindsey, I. C. Schreiman, H. C. Hsu, P. C. Kearney, A. M. Marguerettaz, *J. Org. Chem.* **1987**, *52*, 827–236; b) P. Rothemund, *J. Am. Chem. Soc.* **1935**, *57*, 2010–2011.

[11]   a) N. Kobayashi, R. Kondo, S. Nakajima, T. Osa, *J. Am. Chem. Soc.* **1990**, *112*, 9640–9641; b) Y. Tanaka, W. Hoshino, S. Shimizu, K. Youfu, N. Aratani, N. Maruyama, S. Fujita, A. Osuka, *J. Am. Chem. Soc.* **2004**, *126*, 3046–3047; c) S. Saito, K. S. Kim, Z. S. Yoon, D. Kim, A. Osuka, *Angew. Chem. Int. Ed.* **2007**, *46*, 5591–5593; *Angew. Chem.* **2007**, *119*, 5687–5689.

[12]   Y. Manabe, M. Uesaka, T. Yoneda, Y. Inokuma, *J. Org. Chem.* **2019**, *84*, 9957–9964.

[13]   Y. Tobe, K. Ueda, K. Kakiuchi, Y. Odaira, Y. Kai, N. Kasai, *Tetrahedron* **1986**, *19*, 2184–2185.

[14]   P. A. Gale, J. L. Sessler, V. Král, V. Lynch, *J. Am. Chem. Soc.* **1996**, *118*, 5140–5141.

[15]   Gaussian 16, Revision C.01, M. J. Frisch, G. W. Trucks, H. B. Schlegel, G. E. Scuseria, M. A. Robb, J. R. Cheeseman, G. Scalmani, V. Barone, G. A. Petersson, H. Nakatsuji, X. Li, M. Caricato, A. V. Marenich, J. Bloino, B. G. Janesko, R. Gomperts, B. Mennucci, H. P. Hratchian, J. V. Ortiz, A. F. Izmaylov, J. L. Sonnenberg, D. Williams-Young, F. Ding, F. Lipparini, F. Egidi, J. Goings, B. Peng, A. Petrone, T. Henderson, D. Ranasinghe, V. G. Zakrzewski, J. Gao, N. Rega, G. Zheng, W. Liang, M. Hada, M. Ehara, K. Toyota, R. Fukuda, J. Hasegawa, M. Ishida, T. Nakajima, Y. Honda, O. Kitao, H. Nakai, T. Vreven, K. Throssell, J. A. Montgomery, Jr., J. E. Peralta, F. Ogliaro, M. J. Bearpark, J. J. Heyd, E. N. Brothers, K. N. Kudin, V. N. Staroverov, T. A. Keith, R. Kobayashi, J. Normand, K. Raghavachari, A. P. Rendell, J. C. Burant, S. S. Iyengar, J. Tomasi, M. Cossi, J. M. Millam, M. Klene, C. Adamo, R. Cammi, J. W. Ochterski, R. L. Martin, K. Morokuma, O. Farkas, J. B. Foresman, and D. J. Fox, Gaussian, Inc., Wallingford CT, 2016.

[16]   a) D.-S. Choi, S. Huang, M. Huang, T. S. Barnard, R. D. Adams, J. M. Seminario, J. M. Tour, *J. Org. Chem.* **1998**, *63*, 2646–2655; b) H. M. Gilow, D. E. Burton, *J. Org. Chem.* **1981**, *46*, 2221–2225; c) C. Zonta, F. Fabris, O. D. Lucchi, *Org. Lett.* **2005**, *7*, 1003–1006.

[17]   a) G. Cafeo, F. H. Kohnke, G. L. La Torre, A. J. P. White, D. J. Whilliams, *Angew. Chem. Int. Ed.* **2000**, *39*, 1496–1498; *Angew. Chem.* **2000**, *112*, 1556–1558; b) G. Gafeo, F. H. Kohnke, G. L. La Torre, M. F. Parisi, R. P. Nascone, A. J. P. White, D. J. Williams, *Chem. Eur. J.* **2002**, *8*, 3148–3156.

Entry for the Table of Contents

Calix[1]furan[2]pyrrole   linear intermediate   Calix[2]furan[4]pyrrole
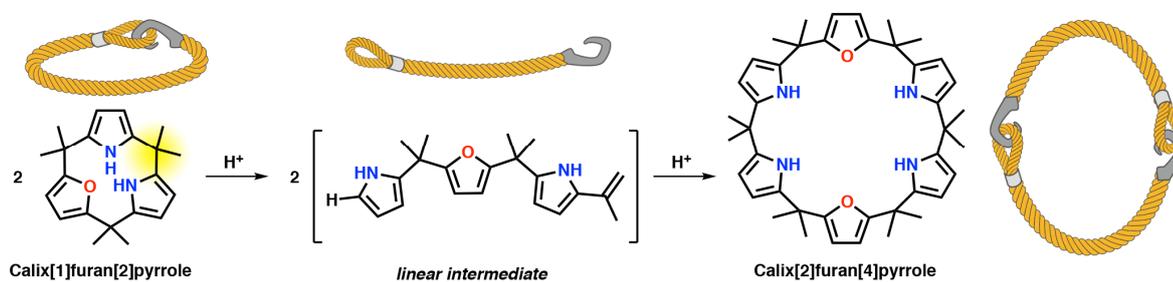
Calix[*n*]furan[3–*n*]pyrroles (*n* = 0~3) were synthesized from cyclicoligoketone precursors to investigate strain-induced macrocyclic ring expansion reactions. As the number of inner NH sites increases, the macrocyclic ring strain increased. Detailed mechanism analysis revealed that calix[6]pyrrole type larger macrocycles were formed through regioselective cleavage and subsequent cyclodimerization of linear intermediates.